Preparation and characterization of porous and electrically conducting carbon–clay composites

TAKAKI KANBARA, TAKAKAZU YAMAMOTO*
Research Laboratory of Resources Utilization, Tokyo Institute of Technology, 4259 Nagatsuta, Midori-ku, Yokohama 227, Japan

HIROYUKI IKAWA
Department of Inorganic Materials, Faculty of Engineering, Tokyo Institute of Technology, 2-12-1 Ookayama, Meguro-ku, Tokyo 152, Japan

TOMOHIKO TAGAWA, HISAO IMAI
Research Laboratory of Engineering Materials, Tokyo Institute of Technology, 4259 Nagatsuta, Midori-ku, Yokohama 227, Japan

Porous and electrically conducting carbon–clay composites were prepared by firing mixtures of carbon powder (0 to 20 wt%) and clay minerals. They showed porosity of 50 to 65% and had high mechanical strength (compressive strength = 130 to 400 $kg\,cm^{-2}$) as well as high resistance against thermal oxidation in air. Their electrical conductivity, σ, increased with increasing carbon content levelling off at about 20 wt% of carbon content to give a σ value of about 2 $S\,cm^{-1}$. Formation of carbon chains is considered to be responsible for the electrical conduction in the composite, and a model to correlate the electrical conductivity with the carbon content has been proposed by modifying a model previously proposed by Scarisbrick.

1. Introduction

Carbon materials are widely used because of their excellent characteristics such as high electrical conductivity and resistance to high temperatures and corrosion. Porous carbon sheets, mats and rods have been used as electrodes of various batteries such as fuel cells and Zn–air batteries [1–4].

Carbon black is especially useful carbon material for the preparation of electrically conducting composites. Carbon black–polymer composites have been extensively studied and a variety of commercial composites have been produced [4–6] however, reports on carbon–ceramic composites have been relatively limited [8–11]. In particular very few reports on the preparation of porous carbon–ceramic composites, their electrical conducting properties, and their applications have been published.

We now report the preparation of porous and electrically conducting carbon–clay composites by firing mixtures of carbon black and clay. Their good physical, chemical and mechanical properties, mean that they seem to have electrical and electronic applications; for example they seem to be useful as electrodes of rechargeable batteries and fuel cells and as shielding materials for electromagnetic waves. This paper deals with the preparation of the composites, their properties including electrical conductivity, porosity, mechanical strength and thermal stability in air, and the electrical conducting mechanism of the composites. Some of the results in this paper have previously been reported in a communication form [12].

2. Experimental details

2.1. Materials and preparation of composites

Starting materials and their main characteristics are listed in Table I. Three types of carbon black, Ketjen black EC (code: KBEC), Ketjen black ECDJ-600 (ECDJ-600), and Toka black #5500 (TB5500), having considerably high surface area were used in this study. Two kinds of clay minerals, Kibushi clay and Roseki clay, which occurred at Sanage in Aichi prefecture and Syokozan in Hiroshima prefecture, respectively, were examined. The clay minerals were ball-milled, and particles smaller than 20 μm were collected by elutriations. Compositions of the clay minerals were examined by using an X-ray diffraction analyser, Phillips Model PS-1051.

Carbon–clay composites, made up of different carbon contents (0 to 23 wt%), were prepared by the following method. A given ratio of carbon black and clay was mixed with distilled water in an agate mortar. Then the mixture was pressed into a pellet, typically of 10 mm diameter and 3 mm thick, at a pressure of about 100 $kg\,cm^{-2}$. The pellet was dried in air for several days and fired in an argon atmosphere to prevent oxidation of the carbon. The firing was performed for 1 h at 800 and 1100° C in a furnace using Kibushi and Roseki clay, respectively. The carbon content (C%) of the fired composites, determined by elemental analysis, showed most (> 98%) of the carbon added was not lost by oxidation during the firing.

The phase changes of the clay minerals after the firing was followed by X-ray diffraction analysis. The

*Author to whom correspondence should be addressed.

0022–2461/89 $03.00 + .12

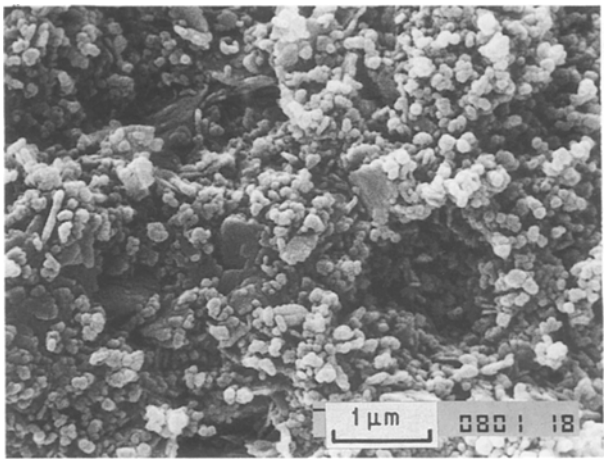

Figure 1 Scanning electron micrograph of sintered KBEC–Kibushi clay composite (C % = 15 wt %). White parts and gray parts are due to carbon powder and the sintered clay, respectively. (× 20 000).

sectional texture of the fired composites was examined by JEOL JSM-T220 Scanning Microscope.

2.2. Measurement of physical properties of the composite

The bulk density of the composite was calculated from its weight and size. The porosity was determined by measurement of the amount of water taken in the composite, and calculated from the following equation

$$\text{Porosity} = (\text{Weight of } H_2O/\text{Volume of composite}) \times 100\% \quad (1)$$

The compressive strength was calculated from a weight loaded perpendicularly to the surface of the samples (5.0 mm diameter and 2.5 mm thickness) just before the sample broke. The weight was measured with a MKS PL-1500 Precision Universal Tester operated at a cross-head speed of 1.0 mm min^{-1}.

Thermogravimetric analysis (TGA) of the composite was carried out in air using a Shimadzu Thermogravimetry Analyser TGA-30 at a temperature elevation rate of 10° C min^{-1}.

The electrical conductivity was measured by a two- or four-point method in an argon atmosphere. In the former method, the electrical conductivity was obtained from a linear *I–V* relationship, whereas in the latter method it was measured using a Hokuto-denko HB-301 potentiostat/galvanostat and a Takeda-riken TR-8651 electrometer. The carbon–clay composite was cut into a bar (about 7.0 mm × 7.0 mm × 2.0 mm), connected to lead wires with silver paste.

The specific surface area of the composite was measured by a BET method [13]. Cyclic voltammetry was carried out using a Hokuto-denko HB-301 potentiostat/galvanostat and a Hokuto-denko HB-104 function generator.

3. Results and discussion

3.1. Structure and composition of composites

X-ray diffraction analysis of the fired specimen indicated that kaolinite of Kibushi clay became amorphous. On the other hand, pyrophyllite of Roseki clay was dehydroxylated and partly changed to mullite. A broad (0 0 2) peak of carbon black was not changed after the firing.

Fig. 1 shows microphotographs of a sintered KBEC–Kibushi clay composite (C % = 15 wt %). Fig. 1 reveals the presence of numerous micropores (< 1.0 μm) and aggregation of carbon black powders to form particles with a diameter of about 100 nm. In the case of the composite prepared by using Roseki clay, the particle size of the fired Roseki clay is larger than that of the fired Kibushi clay and the porosity of the KBEC-Roseki clay composite is higher than that of the KBEC–Kibushi clay composite.

3.2. Physical properties of the composites

3.2.1. Porosity

Fig. 2 shows the dependence of porosity of the fired carbon–clay composites on the wt % of carbon added. As depicted in Fig. 2, the composites have a porosity as high as 50 to 65% when they contain more than 10 to 15 wt % of carbon; the value of porosity being comparable to or higher than the porosity of a commercially available porous carbon plate (Nippon carbon #P140, datum is shown by ▼ in Fig. 2). The porosity of the composite strongly depends on the kind of clay and carbon powder. Use of the Roseki clay gave composites with high porosity, but their mechanical strength was not high. In the case of the carbon–Kibushi clay composites, a trend that makes use of carbon powder with lower density and higher porosity gave the composite with higher porosity was observed.

3.2.2. Mechanical strength

Fig. 3 shows the change of compressive strength of the

TABLE I Starting materials to prepare the composites

Carbon powder	(Code)	Supplier	Particle diameter (nm)	N_2, BET area ($m^2 g^{-1}$)	DBP* volume ($cm^3 g^{-1}$)
Ketjen black EC	(KBEC)	Lion corporation	35	929	3.50
Ketjen black ECDJ600	(ECDJ600)	Lion corporation	38	1270	4.80
Toka black #5500	(TB5500)	Tokai Carbon	25	206	1.55

Clay	(locality)	Composition	SiO_2	Al_2O_3	Fe_2O_3	K_2O
Kibushi clay	(Sanage)	Kaolinite (main) + α-quartz	42–44	37–39	2	0.4
Roseki clay	(Syokozan)	Pyrophyllite (main) + α-quartz + kaolinite	72	23	0.1	0.5

*Determined by mixing the carbon black with dibutylphthalate (DBP) in a Brabender absorptometer.

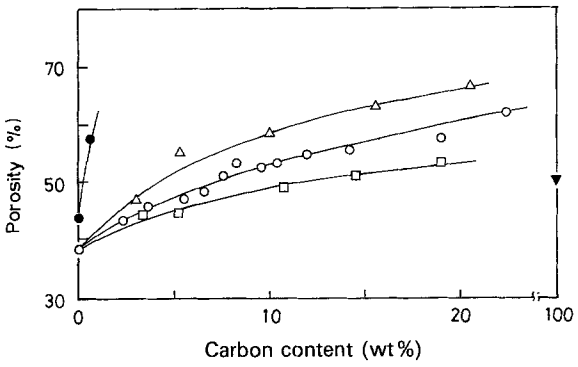

Figure 2 Dependence of porosity of sintered carbon–clay composites on the carbon content. (○) KBEC–Kibushi clay; (△) ECDJ600–Kibushi clay; (□) TB5500–Kibushi clay; (●) KBEC–Roseki clay; (▼) porous carbon plate (Nippon carbon, P#140).

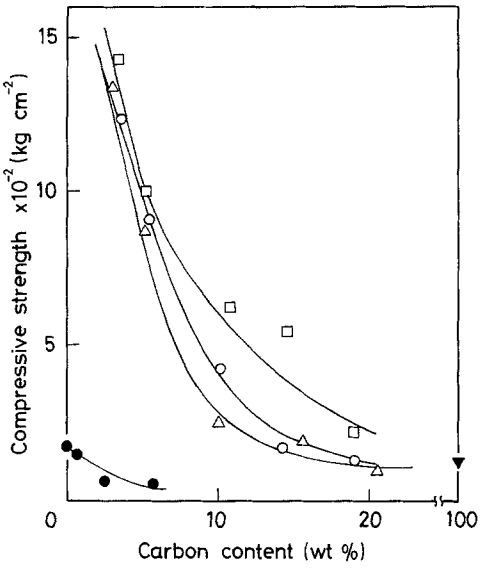

Figure 3 Compressive strength of sintered carbon–clay composites plotted against carbon content. (○) KBEC–Kibushi clay; (△) ECDJ600–Kibushi clay; (□) TB5500–Kibushi clay; (●) KBEC–Roseki clay; (▼) porous carbon plate (as in Fig. 2).

composites with carbon black content. In the case of the carbon–Kibushi clay composites, the compressive strength of the composites decreased with an increase in the carbon content and a decrease in the bulk density of the original carbon black. Even when the carbon–Kibushi clay composite contained 10 to 15 wt % of carbon and consequently the porosity was higher than 40% (cf. Fig. 2), the composite showed a compressive strength greater than 170 kg cm^{-2}, indicating that the fired clay formed a strong framework.

One of the most porous carbon–Kibushi clay composites (carbon black = KBEC, C% = 19 wt %, porosity = 54%) had a compressive strength of 130 kg cm^{-2}, the value being comparable to the compressive strength (130 kg cm^{-2}, shown by a data point (▼) in Fig. 3) of the commercial porous carbon plate (Nippon carbon #P140) having porosity of 50%. These data indicate that the firing temperature (800° C) for the carbon–Kibushi clay composites was high enough to make a mechanically strong framework of fired clay. Raising the firing temperature for the carbon–Kibushi clay composite gave mechanically stronger composites, however it caused a decrease in the porosity of the composite; a firing temperature of 800° C seems to be most suitable for the preparation of a porous composite.

In contrast to the carbon–Kibushi clay composite, the KBEC–Roseki clay composite had a low compressive strength even for a low carbon content. This suggests that the firing temperature (1100° C) was not high enough to form a strong framework with the Roseki clay. Attempts to obtain the composite at a higher temperature were not successful due to partial oxidation of the carbon during firing. Due to the relatively low mechanical strength of the carbon–Roseki clay composites, most of the present research was carried out with carbon–Kibushi clay composites.

3.2.3. Surface area

The fired carbon–Kibushi clay composites showed a large surface area of about 60 to 250 m^2 g^{-1} as shown in Table II. The value of the surface area roughly agrees with calculated value (Table II), according to the following equation.

Calculated area = surface area of original carbon × fraction of carbon + surface area of sintered clay (24.5 m^2 g^{-1}) × fraction of sintered clay (2)

TABLE II Surface area and electrostatic capacitance of the carbon–clay composites

No.	Composite	Carbon content (wt %)	Surface area (m^2 g^{-1})		Electrostatic capacitance[b] (F cm^{-3})
			Found	Calculated[a]	
1	ECDJ600–Kibushi	5.3	86.8	90.6	4.2
2	ECDJ600–Kibushi	10.0	149.1	149.1	6.4
3	ECDJ600–Kibushi	15.6	210.6	218.8	8.4, 9.8[d], 13.1[e]
4	ECDJ600–Kibushi	20.5	243.6	279.8	9.2
5	KBEC–Kibushi	14.2	154.1	152.9	6.9
6	TB5500–Kibushi	14.6	58.9	51.0	2.4
7	Commercial porous carbon (P#140, Nippon carbon[c])	Pure	0.2		0.01

[a] Calculated from Equation 2.
[b] Measured in an aqueous solution containing $ZnCl_2$ (1 M) and KCl (1 M).
[c] See the text.
[d] In an aqueous solution of NaCl (2.5 M).
[e] In an γ-butyrolactone solution of $LiClO_4$ (1 M).

TABLE III Resistivity against air oxidation determined by TGA under air

No.	Sample			Temperature (°C)
	Clay	Carbon black (carbon content/wt %)		
1	None	KBEC (100)	original carbon black	455
2	None	ECDJ600 (100)	original carbon black	545
3	None	TB5500 (100)	original carbon black	505
4	Kibushi	KBEC (19)		560
5	Kibushi	ECDJ600 (20)		560
6	Kibushi	TB5500 (19)		550
7	Porous carbon (P#140[b], from Nippon carbon)			545

[a]Temperature where weight loss of the sample due to the air oxidation started (measured up to 900° C). Rate of temperature rise = 10° C min^{-1}.
[b]See footnote c of Table II.

The coincidence of the observed and calculated values suggests that the microstructures of the carbon black were not changed during the sintering, and chemical and physical properties of the fired clay were not greatly changed by the presence of the carbon powder.

The observed surface area was about 10^3 times larger than the surface area of commercial porous carbon plate (No. 7 in Table II). Due to the large surface area, the composite gave a large electric double-layer capacitance [14–16] in electrolytic solutions as determined by cyclic voltammetry and summarized in the last column of Table II. Details of the measurement of the electric double-layer capacitance and use of the composite as capacitors has been reported elsewhere [17].

3.2.4. Resistivity against air oxidation

The resistivity of carbon in the composite against air oxidation was determined by TGA under air. Table III lists the temperature where weight loss began due to air oxidation. The data in Table III reveal that the resistivity of the carbon powder to air oxidation increases with the composite formation with the clay. Particularly, in the case of the KBEC–Kibushi clay composite (C % = 19 wt %, No. 4 in Table III), the air oxidation of the carbon powder in the composites started at a temperature by 105° C higher than the temperature observed with the original KBEC. Exposure of the two samples to air for 1 h at 480° C demonstrated the large difference in the resistivity of the two samples; the original KBEC completely disappeared by oxidation, whereas the weight loss of the sintered KBEC–Kibushi clay composite was negligible.

Thus, resistivity of the composites to air oxidation becomes comparable to or higher than that of the commercially available porous carbon (No. 7 in Table III), although the composite has a much larger surface area as described above. Due to the high stability and large surface area, the composites will be useful as electrodes used at high temperatures (e.g., electrodes of fuel cells [18]). The improvement of the resistivity to air oxidation is attributed to the protective effects of the ceramic component, similar effects having been reported for carbon–B_4C composites [19].

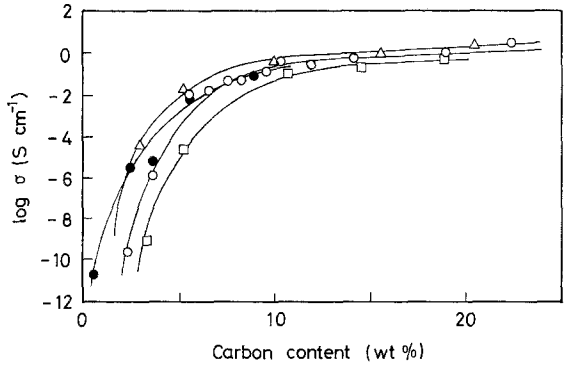

Figure 4 Electrical conductivity of sintered carbon–clay composites at 25° C. (○) KBEC–Kibushi clay; (△) ECDJ600–Kibushi clay; (□) TB5500–Kibushi clay; (●) KBEC–Roseki clay.

3.2.5. Electrical conductivity

Fig. 4 shows the electrical conductivity of the composites plotted against wt % of carbon. The electrical conductivity, σ, increases with an increase in the carbon content, and it levels off at about 20 wt % of carbon to give a σ value of about 2 S cm^{-1} in cases of the KBEC–Kibushi clay and ECDJ600–Kibushi clay composites. The σ value is comparable to reported σ values for various polymer–carbon composites [5–7] with a high content of carbon powder. Among the three kinds of carbon blacks used for the preparation of the carbon–Kibushi clay composites, ECDJ600 gave the composite with the highest σ value at relatively low wt % of carbon (e.g., 5 wt %) and KBEC gave the composite with the second highest σ value. Similar results concerning the effects of the kind of carbon black on the electrical conductivity of the carbon–polymer composites have been reported [7, 20].

In a similar way to the mechanism of electric conduction proposed for the polymer–carbon composites, the electric current in the present carbon–clay composite is considered to flow through carbon chains formed in the composite. Minor temperature dependence (σ(333 K)/σ(203 K) = 1.1) of the electric conductivity as well as small Hall coefficient [21] support this view.

3.2.6. Elucidation of the dependence of the electrical conductivity on the carbon content

Scarisbrick [22] has proposed two equations to express the electric conductivity of composites consisting of electrically conducting particles dispersed in an insulating medium; the electric conduction is considered to originate from the chain of the electrically conducting particles formed in the composite.

One equation is proposed for the composite in which the electrically conducting particles exist in a randomly dispersed distribution, and in this case the electrical conductivity σ is expressed by

$$\sigma = \sigma_0 \times V_f \times P \times C^2 \quad (3)$$

where σ_0 and V_f represent the electrical conductivity of pure conductor and volume fraction of the conducting component, respectively, and the term P (probability of conduction occurring through the bulk material) and C^2 (measurement factor) are related to V_f by

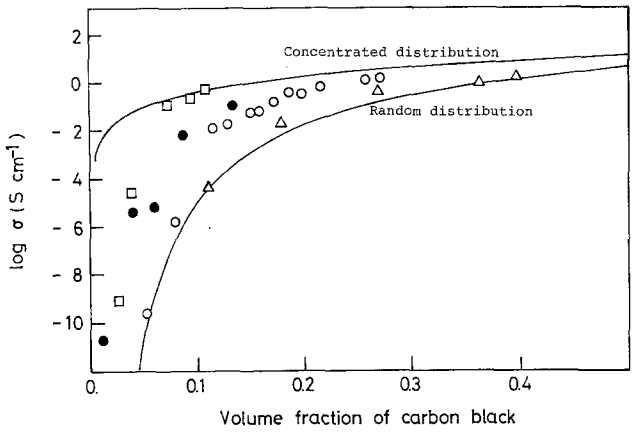

Figure 5 Electrical conductivity of sintered carbon–clay composites as a function of volume fraction of carbon black at 25° C. (○) KBEC–Kibushi clay, (△) ECDJ600–Kibushi clay, (□) TB5500–Kibushi clay; (●) KBEC–Roseki clay, (——) calculated from Equations 3 and 6, respectively.

Equations 4 and 5, respectively

$$P = V_f^{(V_f)^{-2/3}} \quad (4)$$

$$V_f = 3C^2 - 2C^3 \quad (5)$$

Another equation is proposed for the composite in which the electrically conducting particles exist in a concentrated distribution. In this case the term P in Equation 3 becomes 1 at any value of V_f and the σ value is expressed by

$$\sigma = \sigma_0 \times V_f \times C^2 \quad (6)$$

Fig. 5 shows the electrical conductivity, σ, of the four types of composites as a function of volume fraction of the carbon black, V_f, and the two theoretical curves calculated according to Equations 3 and 6. In the calculation, the σ_0 value was taken as 1×10^2 S cm^{-1} [23] and the V_f values were calculated from

$$V_f = \varrho_{total} \times (C\%/100)/\varrho_c \quad (7)$$

where ϱ_{total} and ϱ_c represent the bulk density of the composite and the original carbon black, respectively, and C % refers to carbon content (wt %).

In Fig. 5, the ECDJ600–Kibushi clay composites give data which can almost be explained by assuming random distribution. However, the other data obtained for the other three types of composites lie between the two theoretical curves. In order to explain the relationship between electrical conductivity and volume fraction of carbon black, we modify Scarisbrick's theoretical equations.

3.2.6.1. Modification 1. The first modification is concerned with the probability term P. Instead of the completely random structure (P given by Equation 4) and the completely concentrated structure ($P = 1$), we consider of an intermediate concentrated structure. The probability term P is now assumed to be given by

$$P = \alpha \times (V_f)^{(V_f)^{-2/3}} \quad (P \leqslant 1) \quad (8)$$

In this equation the probability expressed by Equation 4 is multiplied by a factor, α, and the value of α is taken as a measure of the ease of formation of the concentrated structure of carbon black. When the probability term P is expressed by Equation 4, the dependence of P on V_f is expressed by curve a in Fig. 6. In the case of the completely concentrated structure, P equals 1 (d in Fig. 6). On the other hand, by choosing a value of between α 3 and 23, one obtains curves b and c in Fig. 6.

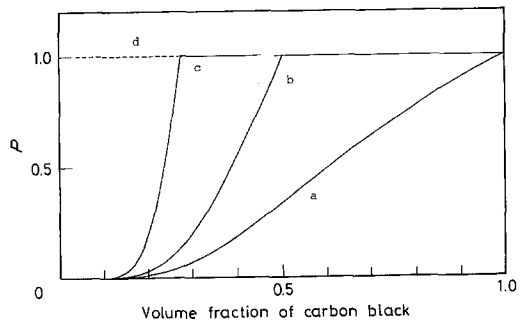

Figure 6 Probability term P calculated according to Equations 4 and 8. (a) Calculated according to Equation 4 ($\alpha = 1$ in Equation 8); (b) calculated according to Equation 8 ($\alpha = 3$); (c) calculated according to Equation 8 ($\alpha = 23$); (d) the case of ideally concentrated structure ($\alpha = \infty$).

3.2.6.2. Modification 2. Scarisbrick's equation has been proposed for non-porous composites. However, the carbon–clay composites show high porosity (Fig. 7). This suggests that some modification of V_f may be necessary. Thus, we introduce the following parameter β

$$V_f' = V_f + \beta \quad (9)$$

3.2.6.3. Curve fitting and values of α and β. According to the modifications described above, the electrical conductivity, σ, is expressed by

$$\sigma = \sigma_0 \times (V_f + \beta) \times P' \times C'^2 \quad (10)$$

where

$$P' = \alpha(V_f + \beta)^{(V_f+\beta)^{-2/3}} \quad P \leqslant 1 \quad (11)$$

$$V_f + \beta = 3C'^2 - 2C'^3 \quad (12)$$

From Equation 10, we used non-linear least-squares

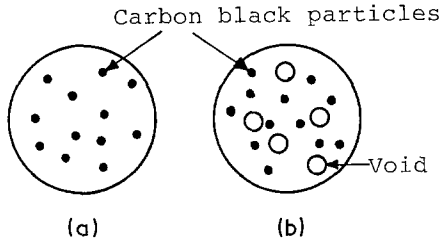

Figure 7 Arrangement of carbon powder in composite. (a) Non-porous composite; (b) porous composite like the sintered carbon–clay composite.

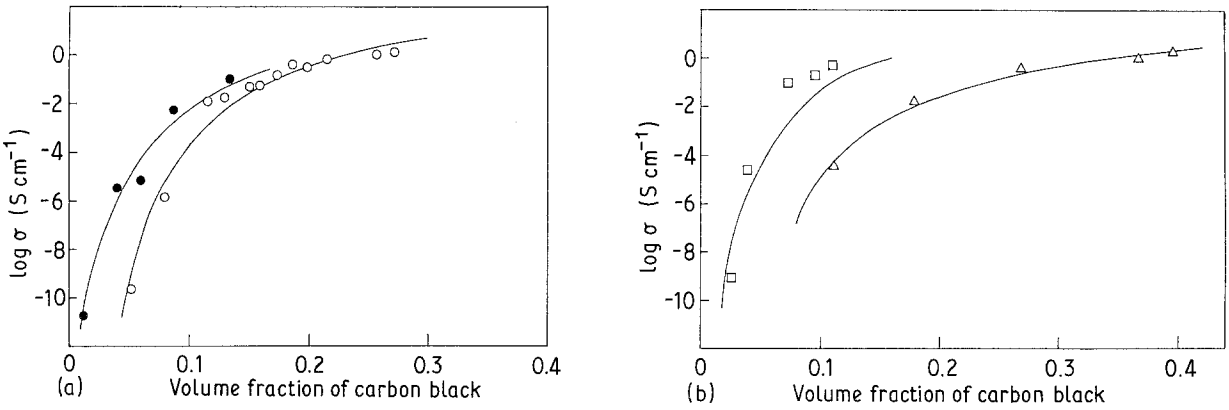

Figure 8 Curve fitting of the electrical conductivity of the sintered carbon–clay composites. (a) (○) KBEC–Kibushi clay, (●) KBEC–Roseki clay. (b) (△) ECDJ600–Kibushi clay, (□) TB5500–Kibushi clay. Curves are calculated from Equation 10 using the α and β values in Table IV.

regression. Its results are shown in Figs 8a and b, and the values of α and β thus obtained are summarized in Table IV. As shown in Fig. 8, the experimental data approximately lie on the calculated curves.

The α value mainly depends on the kind of carbon black (Table IV). Use of KBEC in both the composites with Kibushi and Roseki clay gave almost the same α value. On the other hand, use of ECDJ600 and TB5500 afforded considerably different α values. These results suggest that the ease of formation of the concentrated structure of carbon black is mainly determined by the properties of carbon black itself and the kind of clay affects it to only a minor extent.

The β value, on the other hand, depends on both the kind of clay minerals and that of carbon black. When KBEC or ECDJ600 which has a hollow shell structure is used in combination with the Kibushi clay which forms a mechanically strong framework under the firing conditions, the β value is zero (1 and 2 in Table IV). On the other hand, when TB5500 which does not have a hollow structure or Roseki clay which does not form the mechanically strong framework is used, the curve fitting gives the β value of about 0.3 (3 and 4 in Table IV).

3.2.7. Passing of gas and liquid through the composite

Gases passed through the porous composite. However, the rate of flow of gas was rather low since the diameter of the micropores in the composite was small (1 μm, cf. Fig. 1) and it caused large flow resistance. When a composite with a diameter ϕ = 5 mm and length = 2 mm (Fig. 9) was used and oxygen flowed through the composite along a direction perpendicular to the surface of the composite; the flow rate of oxygen changed with a change of applied oxygen pressure as shown in Fig. 10. If we apply the Hagen–Poiseuilli law

$$\text{Rate of flow} = (\pi r^4/8\eta l)\Delta P \qquad (13)$$

TABLE IV Values of α and β calculated from the curve fitting

No.	Sample	α	β
1	KBEC–Kibushi	22.7	0
2	ECDJ600–Kibushi	1.7	0
3	TB5500–Kibushi	259.5	0.27
4	KBEC–Roseki	18.8	0.33

where r is the radius of micropore, η the viscosity, l the length of micropore and ΔP the applied pressure, and assume that the composite has micropores as shown in Fig. 9 and porosity of 50%, we obtain the broken line in Fig. 10 for the dependence of the calculated rate of flow of oxygen on the applied pressure. As shown in Fig. 10, the calculated value roughly agrees with the observed value, supporting the validity of the model shown in Fig. 9.

The rate of flow of liquid materials such as water and hydrocarbons was very low due to their high viscosity. Since gas can pass through the composite at an appropriate rate of flow and the passing of water is negligible, the present composite is suited for electrodes of fuel cells using gases as active materials, and use of the composites for the electrodes will be reported elsewhere.

4. Conclusion

Electrically conducting carbon–clay composites having high porosity, high mechanical strength, and high resistivity to air oxidation were prepared by firing mixtures of carbon and clay. The relation between electrical conductivity and carbon content of the composites can be elucidated by the modified Scarisbrick's

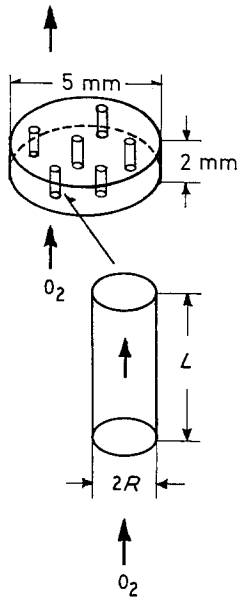

Figure 9 A model for calculation of rate of flow of gas through the composite. (Porosity = 50%, R = 0.5 μm, L = 2.0 mm).

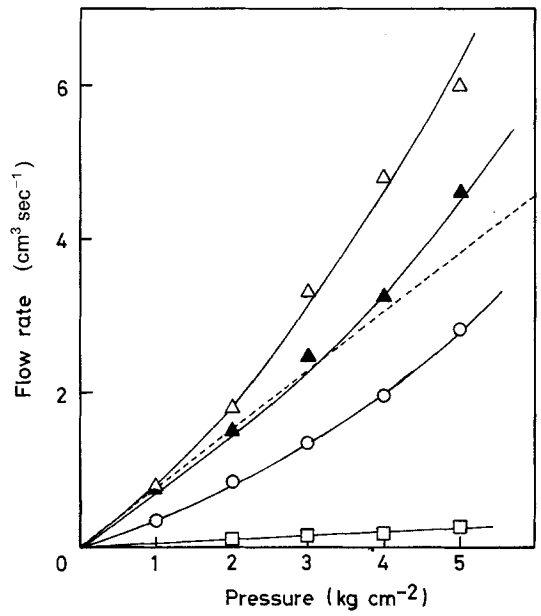

Figure 10 Flow rate of oxygen through the porous composites. (△) ECDJ600–Kibushi clay (C % = 20.5 wt %); (▲) ECDJ600–Kibushi clay (C % = 15.6 wt %); (○) KBEC–Kibushi clay (C % = 19.0 wt %); (□) TB5500–Kibushi clay (C % = 19.0 wt %). (----) Calculated from Equation 13 for the model shown in Fig. 9.

model. Owing to their high porosity, electrically conducting properties, and large surface area, they seem to find some applications for example, the electrodes of $Zn–I_2$ and $Zn–O_2$ batteries [25] and the electrodes of electric double layer capacitors [17]. Use of other carbon powder and clays like artificial clays [26] will afford similar composites having interesting characteristics.

References

1. E. ROYAIE and J. JORNE, *J. Electrochem. Soc.* **132** (1985) 1273.
2. J. JORNE and E. ROAYAIE, *ibid.* **133** (1986) 697.
3. R. HOLZE and W. VIELSTICH, *J. Electrochem. Soc.* **131** (1984) 2298.
4. K. MICKA and I. ROUSAR, *Electrochim. Acta* **29** (1984) 1411.
5. K. MIYASAKA, K. WATANABE, E. JOJIMA, H. AIDA, M. SUMITA and K. ISHIKAWA, *J. Mater. Sci.* **17** (1982) 1610.
6. S. MIYAUCHI and E. TOGASHI, *J. Appl. Polym. Sci.* **30** (1985) 2743.
7. A. A. GHANI, A. I. EATAH, A. A. HASHEM and H. HASSAN, *Angew. Makromol. Chem.* **129** (1985) 1.
8. K. MIYAZAKI, T. HAGIO and K. KOBAYASHI, *J. Mater. Sci.* **16** (1981) 752.
9. A. OYA, *Nendo Kagaku* **26** (1986) 157.
10. B. R. MICCIOLI, *Amer. Ceram. Soc. Bull.* **45** (1966) 670.
11. L. A. GEL'FOND, V. S. DERGUNOVA and YU. N. PETROV, *Sov. Powder Metall. Metal Ceram.* **15** (1976) 225.
12. T. KANBARA, T. YAMAMOTO, H. IKAWA, T. YAGAWA and H. IMAI, *J. Mater. Sci. Lett.* **6** (1987) 1195.
13. G. M. BARROW, "Physical Chemistry" (McGraw-Hill International, New York, 1979) p. 744.
14. A. NISHINO, A. YOSHIDA, I. TANAHASHI, I. TAJIMA, M. YAMASHITA, T. MURANAKA and H. YONEDA, National Technical Report, **31** (1985) 318.
15. S. SEKIDO, T. MURANAKA, Y. YOSHINA and H. MORI, *ibid.* **26** (1980) 220.
16. T. MURANAKA and H. MORI, *Denshi Zairyo* **18** (1979) 65.
17. T. KANBARA, T. YAMAMOTO, K. TOKUDA and K. AOKI, *Chem. Lett.* (1987) 2173.
18. D. LINDEN, "Handbook of Batteries and Fuel Cells" (McGraw-Hill Book Company, New York, 1984).
19. K. MIYAZAKI, T. HAGIO and K. KOBAYASHI, *Tanso (Carbon)* **111** (1982) 141.
20. D. N. BIGG, *J. Rheology* **28** (1984) 501.
21. A. R. UBBELODE and F. A. LEWIS, "Graphite and its Crystal Compounds" (Clarendon, Oxford, 1960).
22. R. M. SCARISBRICK, *J. Phys. D* **6** (1973) 2098.
23. A. R. BLYTHE, "Electrical Properties of Polymers" (Cambridge University Press, Cambridge, UK, 1979).
24. W. F. VERHELST, K. G. WOLTHUIS, A. VOET, P. EHRURGER and J. B. DONNET, *Rubber Chem. Technol.* **50** (1977) 735.
25. T. YAMAMOTO and T. KANBARA, *Inorganica Chimica Acta* **142** (1988) 191.
26. W. YU and D. WANG, *Solid State Commun.* **63** (1987) 1041.

Received 15 March
and accepted 28 July 1988